Bull. Chem. Soc. Jpn., 72, 265—277 (1999)

Photoisomerizable DNA Ligands. Spectral and Electrochemical Properties and Base-Pair Selectivity of Binding of Bis[2-(1-alkylpyridinium-4-yl)vinyl]benzene Dyes

Bernard Juskowiak,*,# Mitsuyoshi Ohba, Masao Sato, Shigeori Takenaka, Makoto Takagi, and Hiroki Kondo†

Department of Chemical Systems and Engineering, Graduate School of Engineering, Kyushu University, Fukuoka 812-8581

†Department of Biochem. Eng. Sci., Kyushu Institute of Technology, Iizuka 820

(Received July 2, 1998)

A series of bis[2-(alkylpyridinium-4-yl)vinyl]benzene ligands has been prepared and characterized, and their interactions with DNA have been studied by a combination of spectroscopic, hydrodynamic, and biochemical methods. Although bis[2-(1-alkylpyridinium-4-yl)vinyl]benzene ligands interact with DNA by both groove binding and the intercalation mode, the resulting complexes have different binding characteristics, depending on the nature of the DNA. Unexpectedly, nonplanar *E,Z* isomer also binds to DNA with binding features resembling those of the *E,E* isomer, though with lower affinity. The interaction of both isomers with a minor groove of $[poly(dA\text{-}dT)]_2$ resulted in the formation of more stable complexes compared to the intercalation complexes formed with $[poly(dG\text{-}dC)]_2$. Small differences in the binding parameters between planar *E,E* and non-planar *E,Z* isomers were explained in terms of an incomplete insertion of a dye molecule in the minor groove (AT polymer) or intercalation pocket (GC polymer), thus allowing *trans–cis* isomerization of the protruding arm of the molecule to occur without any dramatic changes in the binding affinity of the ligand. The primary redox activity combined with photophysical features of dyes resulted in a photocleavage of supercoiled circular DNA, which occurred at neutral pH under irradiation with visible light, leading mainly to single-strand nicking.

Some cationic molecules bind readily to nucleic acids and display a variety of interesting biological properties, including antiviral and anticancer activity.[1] They are also widely used as nucleic acid structural probes.[1] Generally, their binding interactions with nucleic acids are classified under four distinct modes: (i) intercalation, (ii) minor-groove binding, (iii) major-groove biding, and (iv) external binding by electrostatic attraction. The intercalation binding mode has been extensively studied and is rather well understood.[2] One of the interesting groups of intercalators includes viologen structure-related derivatives, e.g., diazapyrenium[3] or pheathridinium[4] cations, which show remarkable binding affinity to both double-strand and single-strand DNA. The photoactivity of these compounds, accompanied by advantageous redox properties, were acknowledged in photophysical studies;[5] the efficient quenching of a photoexcited ligand by electron transfer from adjacent nucleobases was commonly reported,[3—5] the electron transfer couples with other dyes as an electron donor and viologens as the acceptor have been used to prove the electron conductivity of the DNA helix.[6—8] Finally, their usefulness as photonucleases capable of DNA strand scission upon exposure to visible light has been reported.[3,4,9,10]

Recently, Wilson's group reported on examples of interesting ligands containing unfused aromatic rings as a structural framework.[11,12] This class of compounds is believed to interact with DNA involving all four binding modes listed above. Their structural similarity to netropsin and other minor groove binders results in very strong interactions with AT-sequences of DNA. The GC-rich regions contain the amino groups from guanine in minor groove, which results in a significant reduction of their groove-binding affinity, and the dyes can bind instead at GC sequences by the intercalation mode. The AT specificity of these drugs is explained by the interplay of such factors as (i) the radius of curvature along the long axis of the dye molecule, (ii) hydrogen bonding between the dye and the floor of minor groove, (iii) positive charge of the dye, enabling strong interactions with minor groove having negative potential, and (iv) van der Waals interactions. Almost all synthetic and naturally occurring groove binders possess all of the above-listed features. The contribution from particular factors to the stabilizing effect for a DNA-dye complex varies, depending on the structural characteristics of the dye. For example, for a family of drugs called lexitropsins, it was shown that beside hydrogen bonding, a cationic character of the ligand is also very important.[13] On the other hand, Wilson et al. pointed out the domination of van der Waals interactions to electrostatic attraction for

Permanet address: A. Mickiewicz Univ., Poznan, Poland.

benzimidazole containing ligands.[14] It must be emphasized, however, that the biding modes of these ligands are still far from being fully understood.

We report here on a new class of DNA-interacting ligands, bis[2-(1-alkylpyridinium-4-yl)vinyl]benzene derivatives, hereafter named simply distilbazolium ligands, since they may be regarded as being two structural entities of a well known stilbazolium derivative, 2-(1-alkylpyridium-4-yl)vinylbenzene, with a common benzene nucleus. They are supposed to exhibit unique binding characteristics of unfused aromatic ligands and advantageous photophysical and redox properties of viologen-related intercalators. The ligands are featured by a linear structure containing two pyridinium moieties bridged by an extended π-electronic system; however, unlike Wilson's ligands, they do not have any hydrogen-bonding formation abilities. Moreover, due to the presence of a delocalized π-electronic system, they may generally be regarded as being planar molecules. However, the presence of two ethylene bridges, which may undergo *trans–cis* photoisomerization, introduces another interesting aspect concerning the behavior of these ligands. Photoisomerization is expected to affect their binding affinity to DNA, and may serve as a unique source of information connected with the preferences in the binding modes. Another interesting feature of distilbazolium ligands is their functional similarity to viologen-related dyes. Although the two pyridinium rings are separated by a π-electronic bridge, the ligands are expected to possess advantageous redox properties suitable for electron-transfer interactions with DNA and for photocleavage activity. We have already reported on the results of preliminary studies concering the binding affinity of the dyes to calf thymus DNA and synthetic oligonucleotides, [poly(dA-dT)]$_2$ and [poly(dG-dC)]$_2$,[15,16] but have subsequently discovered that initial samples of compounds contained a mixture of *trans* and *cis* isomers of unknown composition. Revised binding studies concerning particular isomers, together with other data obtained using other techniques, are reported here. The syntheses of dyes and their fundamental characteristics are also included.

Experimental

Materials. Syntheses of distilbazolium ligands were carried out using an aldol strategy, as shown in Scheme 1. It requires a pyridinium derivative with an activated methyl substituent toward the base-catalyzed aldol condensation with a respective aromatic dialdehyde. The pyridinium salt was prepared from 4-picoline and alkyl iodide or bromide. This procedure provided final products with all trans stereochemistry, as indicated by the ^{1}H NMR coupling (J = 16.5 Hz).

1,4-Dimethylpyridinium Iodide (1). 4-Picoline (3.9 ml, 41.6 mmol) was dissolved in 10 ml of isopropyl alcohol, methyl iodide (2.5 ml, 40.2 mmol) was added, and the mixture was heated for 2 h under reflux. After being cooled to room temperature, the crystalline was collected, washed with diethyl ether, and finally recrystallized from 2-propanol to give 1,4-dimethylpyridinium iodide (6.6 g, 69%; mp 152—153 °C, lit, 144 °C[17]). ^{1}H NMR (250 MHz, $CDCl_3$) δ_H = 2.69 (3H, s, 4-Me), 4.64 (3H, s, N^+Me), 7.90 (2H, d, J = 7.1 Hz, H-3, H-5), 9.15 (2H, d, J = 7.1 Hz, H-2, H-6).

1,4-Dimethylpyridinium Bromide (2). 4-Picoline (40 ml, 0.41 mol) was dissolved in 100 ml of diethyl ether, methyl bromide (20 ml, 0.76 mol) was added, and the stirred mixture was allowed to react at room temperature for 22 h. The precipitated crystalline product was collected, washed with diethyl ether, and finally recrystallized from acetonitrile to give 1,4-dimethylpyridinium bromide (56.4 g, 77%; mp 172—174 °C). ^{1}H NMR (250 MHz, DMSO-d_6) δ_H = 2.60 (3H, s, 4-Me), 4.28 (3H, s, N^+Me), 7.96 (2H, d, J = 6.5 Hz, H-3, H-5), 8.83 (2H, d, J = 6.5 Hz, H-2, H-6).

General Procedure for Other 1-Alkyl-4-methylpyridinium Bromides. 4-Picoline (3.9 ml, 41.6 mmol) was dissolved in 5 ml of isopropyl alcohol. An alkyl bromide (40 mmol) was added, and the mixture was heated for 3 h under reflux. The solvent was evaporated and a waxy residue was dried in a vacuum, followed by washing with hexane and ethyl acetate. The resulting gel was dried in a vacuum to give final 1-alkyl-4-methylpyridinium bromides with yields ranging from 60—80%.

4-Methyl-1-propylpyridinium Bromide (3). ^{1}H NMR (250 MHz, $CDCl_3$) δ_H = 1.02 (3H, t, J = 7.3 Hz, CH_3), 2.10 (2H, sextet, J = 7.3 Hz, CH_2), 2.70 (3H, s, 4-Me), 4.90 (2H, t, J = 7.3 Hz, N^+CH_2), 7.96 (2H, d, J = 6.2 Hz, H-3, H-5), 9.49 (2H, d, J = 6.2 Hz, H-2, H-6).

1-Isopropyl-4-methylpyridinium Bromide (4). ^{1}H NMR (60 MHz, $CDCl_3$) δ_H = 1.73, 1.86 (6H, d, CH_3), 2.72 (3H, s, 4-Me), 5.50 (1H, m, N^+CH), 8.05 (2H, d, J = 6.5 Hz, H-3, H-5), 9.60 (2H,

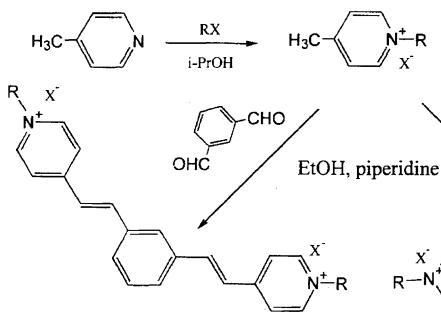

comp.	1	2	3	4	5
R	CH_3	CH_3	nC_3H_7	iC_3H_7	iC_5H_9
X	I	Br	Br	Br	Br

comp.	10a	10b	10c
R	CH_3	CH_3	CH_3
X	I	Br	PF_6

comp.	6	7	8	9
R	CH_3	nC_3H_7	iC_3H_7	iC_5H_9
X	I	Br	Br	Br

Scheme 1.

d, J = 6.5 Hz, H-2, H-6).

1-Isopentyl-4-methylpyridinium Bromide (5). ^{1}H NMR (60 MHz, $CDCl_3$) δ_H = 0.90, 1.00 (6H, d, CH_3), 1.46—2.10 (3H, m, CH, CH_2), 2.66 (3H, s, 4-Me), 4.90 (2H, t, N^+CH_2), 7.98 (2H, d, J = 6.5 Hz, H-3, H-5), 9.47 (2H, d, J = 6.5 Hz, H-2, H-6).

General Procedure for Aldol Condensation. *N*-Alkyl-4-picolinium salt (16 mmol) in 50 ml of ethanol and benzenedicarbaldehyde (8 mmol) were heated under reflux for 22 h with piperidine (few drops) used as a catalyst. After being cooled to room temperature, the precipitate was collected by filtration, washed with hot diethyl ether, and dried under reduced pressure. The crude crystalline product was dissolved in ethanol, worked up with charcoal, and recrystallized from ethanol, or precipitated from ethanol solution with ether.

1,4-Bis[2-(1-methylpyridinium-4-yl)vinyl]benzene Diiodide (6). Yield 47%, mp > 300 °C. Found: C, 43.75; H, 3.89; N, 4.58%. Calcd for $C_{22}H_{22}I_2N_2$: C, 46.50; H, 3.90; N, 4.93%. ^{1}H NMR (500 MHz, DMSO-d_6) δ_H = 4.28 (6H, s, N^+Me), 7.64 (2H, d, J = 17 Hz, H-vinylic), 7.88 (4H, s, benzene H), 8.05 (2H, d, J = 17 Hz, H-vinylic), 8.25 (4H, d, J = 6.5 Hz, H-3, H-3′, H-5, H-5′), 8.88 (4H, d, J = 6.5 Hz, H-2, H-2′, H-6, H-6′).

1,4-Bis(2-[1-propylpyridinium-4-yl)vinyl]benzene Dibromide (7). Yield 10%, mp > 300 °C. Found: C, 57.57; H, 5.50; N, 5.14%. Calcd for $C_{26}H_{30}$ Br_2N_2: C, 58.88; H, 5.70; N, 5.28%. ^{1}H NMR (250 MHz, DMSO-d_6) δ_H = 0.91 (6H, t, J = 7.3 Hz, CH_3), 1.96 (4H, sextet, J = 7.2 Hz, CH_2), 4.51 (4H, t, J = 7.2 Hz, N^+CH_2), 7.72 (2H, d, J = 16.4 Hz, H-vinylic), 7.82 (4H, s, benzene H), 8.12 (2H, d, J = 16.4 Hz, H-vinylic), 8.31 (4H, d, J = 6.5 Hz, H-3, H-3′, H-5, H-5′), 9.03 (4H, d, J = 6.5 Hz, H-2, H-2′, H-6, H-6′).

1,4-Bis(2-[1-isopropylpyridinium-4-yl)vinyl]benzene Dibromide (8). Yield 42%, mp > 300 °C. Found: C, 56.49; H, 5.80; N, 5.06%. Calcd for $C_{25}H_{30}Br_2N_2$: C, 58.88; H, 5.70; N, 5.28%. ^{1}H NMR (500 MHz, DMSO-d_6) δ_H = 1.62 (12H, d, CH_3), 4.94—4.99 (2H, m, N^+CH), 7.69 (2H, d, J = 16.4 Hz, H-vinylic), 7.90 (4H, s, benzene H), 8.12 (2H, d, J = 16.4 Hz, H-vinylic), 8.30 (4H, d, J = 6.5 Hz, H-3, H-3′, H-5, H-5′), 9.10 (4H, d, J = 6.5 Hz, H-2, H-2′, H-6, H-6′).

1,4-Bis[2-(1-isopentylpyridinium-4-yl)vinyl]benzene Dibromide (9). Yield 37%, mp > 300 °C. Found: C, 58.69; H, 6.90; N, 4.55%. Calcd for $C_{30}H_{38}Br_2N_2$: C, 61.44; H, 6.53; N, 4.78%. ^{1}H NMR (500 MHz, DMSO-d_6); δ_H = 0.95 (12H, d, CH_3), 1.59—1.64 (2H, m, CH), 1.81—1.86 (4H, q, CH_2), 4.55 (4H, t, N^+CH_2), 7.66 (2H, d, J = 16.4 Hz, H-vinylic), 7.89 (4H, s, benzene H), 8.09 (2H, d, J = 16.4 Hz, H-vinylic), 8.29 (4H, d, J = 6.5 Hz, H-3, H-3′, H-5, H-5′), 9.02 (4H, d, J = 6.5 Hz, H-2, H-2′, H-6, H-6′).

1,3-Bis[2-(1-methylpyridinium-4-yl)vinyl]benzene Diiodide (10a). Yield 29%, mp > 300 °C. Found: C, 46.33; H, 3.96; N, 4.85%. Calcd for $C_{30}H_{38}Br_2N_2$: C, 46.50; H, 3.90; N, 4.93%. ^{1}H NMR (250 MHz, DMSO-d_6) δ_H = 4.30 (6H, s, N^+Me), 7.63 (1H, t, benzene H-5), 7.74 (2H, d, J = 16.4 Hz, H-vinylic), 7.83 (2H, d J = 7.7 Hz, benzene H-4, H-6), 8.10 (2H, d, J = 16.4 Hz, H-vinylic), 8.25 (1H, s, benzene H-2), 8.30 (4H, d, J = 6.7 Hz, H-3, H-3′, H-5, H-5′), 8.93 (4H, d, J = 6.7 Hz, H-2, H-2′, H-6, H-6′).

1,3-Bis[2-(1-methylpyridinium-4-yl)vinyl]benzene Dibromide (10b). The condensation reaction was carried out at room temperature for 2 h, since prolonged heating yielded a complex reaction mixture that was difficult to purify. Yield 19%, mp > 300 °C. Found: C, 53.09; H, 4.84; N, 5.68%. Calcd for $C_{22}H_{22}Br_2N_2$; C, 55.72; H, 4.68; N, 5.91%. ^{1}H NMR (250 MHz, DMSO-d_6) δ_H = 4.30 (6H, s, N^+Me), 7.62 (1H, t, benzene H-5), 7.70 (2H, d, J = 16.4 Hz, H-vinylic), 7.82 (2H, d, J = 8.2 Hz, benzene H-4, H-6), 8.10 (2H, d, J = 16.4 Hz, H-vinylic), 8.26 (1H, s, benzene H-2), 8.31 (4H, d, J = 6.7 Hz, H-3, H-3′, H-5, H-5′), 8.94 (4H, d, J = 6.7 Hz, H-2, H-2′, H-6, H-6′).

1,3-Bis[2-(1-methylpyridinium-4-yl)vinyl]benzene Bis(hexafluorophosphate) (10c). An anion-exchange reaction was carried out in an aqueous solution of **10b**, 0.2 g (0.35 mmol), and ammonium hexafluorophosphate, 1 g, (6.1 mmol). The precipitate was separated by filtration, washed with cold water, and dried under reduced pressure. Yield 99%, mp > 300 °C. Found: C, 43.69; H, 3.67; N, 4.54%. Calcd for $C_{22}H_{22}F_{12}N_2P_2$: C, 43.72; H, 3.67; N, 4.64%. ^{1}H NMR (250 MHz, DMSO-d_6) δ_H = 4.30 (6H, s, N^+Me), 7.64 (1H, t, benzene H-5), 7.70 (2H, d, J = 16.5 Hz, H-vinylic), 7.84 (2H, d, J = 7.8 Hz, benzene H-4, H-6), 8.06 (2H, d, J = 16.5 Hz, H-vinylic), 8.10 (1H, s, benzene H-2), 8.25 (4H, d, J = 6.7 Hz, H-3, H-3′, H-5, H-5′), 8.90 (4H, d, J = 6.7 Hz, H-2, H-2′, H-6, H-6′).

Calf thymus DNA (ct-DNA) was purchased from Sigma Chemical Co. and was purified as previously described.[18] Ethidium bromide, Hoechst 33258, [poly(dA-dT)]$_2$, [poly(dG-dC)]$_2$, and pBR322 were also purchased from Sigma, and were used without further purification. The supercoiled circular plasmid DNA for viscometric titration of 15.5 kbp was made of vector YEp13 and a portion of yeast genomic insert DNA. This plasmid was propagated in *Escherichia coli* and isolated by a standard method. All of the experiments were conducted in a HEPES buffer (10 mM 2-[4-(2-hydroxyethyl)-1-piperazinyl]ethanesulfonic acid, pH 7.2). Sodium chloride was added to obtain the desired salt concentration. A Milli-Q filtered water (Millipore Co.) was used throughout.

Methods. ^{1}H NMR specta were recorded on a JEOL PMX60SI, Bruker AC250P, or JEOL GSX-400 spectrometer operating at 60, 250, and 400 MHz, respectively, using tetramethylsilane (TMS) as an internal standard. The absorption spectra were recorded with Hitachi U-3210 and 3300 spectrophotometers equipped with a SPR 10 temperature controller. Steady-state fluorescence measurements were carried out using Hitachi 650-60 and F-4010 spectrofluorimeters with excitation- and emission-band widths of 5 nm. The cell compartments were thermostated at 25 °C. All of the measurements were carried out using a 10 mm quartz cell, and the spectra were corrected at the 280—600 nm range using Rhodamine B as a photon counter (a microprocessor operated correction mode). The apparent fluorescence quantum yields of the photoequilibrated samples containing the mixture of isomers (ϕ_{obs}) were determined using quinine sulfate in 0.5 M H_2SO_4 (1 M = 1 mol dm^{-3}) as a quantum yield standard (ϕ^R = 0.545), according to the conventional equation.[19] The quantum yields of free *EZ* and *EE* isomers were determined according to a method described elsewhere.[20] The circular dichroism spectra were recorded in the 230—700 nm spectral range on a JASCO J7200 spectropolarimeter.

Photoisomerization Experiments An aqueous dye solution (100 μM) was irradiated in a thermostated (25 °C) cell compartment of a spectrofluorimeter equipped with a 150 W Xe lamp at a selected wavelength. Nitrogen was purged through the solution during irradiation, and aliquots of 30 μl were removed at desired time intervals and analyzed on a LaChrom HPLC system (Hitachi) composed of an L-7300 column oven, a dual L-7100 pump system, an L-7450H diode array detector, and a D-7000 HPLC interface. Separations were carried out at 30 °C on an InertSil ODS 3 column, (d_p = 5 μm, 250×4.6 mm i.d. (G1 Science Inc.)) with gradient elution. The eluent (10 mM NaCl (A) and MeOH (B)) was run in a linear gradient of 10—60% of B in 25 min at a flow rate of 1.0 ml min^{-1}.

Spectrophotometric Titration. A typical titration consisted of

successive replacements of small amounts (2—4 μl) of a 5 μM solution of dye in a buffer (containing desired NaCl concentration) by the same volume of concentrated DNA solution containing a buffer and a dye, followed by stirring, thermal equilibration, and recording of the spectrum. The data represented as a binding isotherm, were fitted to the simple Scatchard equation[21] and to the McGhee-von Hippel site-exclusion model.[22] A solution of *E,E* isomer (*trans*) was prepared by directly dissolving a solid sample of the dye in water, while an *E,Z* isomer (*cis*)-rich sample was prepared by 30 min irradiation of an *E,E* isomer solution (5 μM) at 410 nm in the sample holder of a spectrofluorimeter equipped with a Xe lamp. Nitrogen gas was purged during irradiation. This procedure enabled us to achieve the photostationary state (pss) with a composition of 80% of the *E,Z* isomer of the dye.[20] To calculate binding data for the *E,Z* isomer, the apparent absorbance values were corrected for the presence of the *E,E* component by subtracting the spectral contribution corresponding to a 1 μM solution of the *E,E* isomer.

Viscosity Titration. Titrations were carried out with a PC-controlled automatic system (Lauda) equipped with a capillary Ubbelohde-type viscometer, automatic pump/stop-watch unit, and thermostated water bath at 30±0.1 °C. Small amounts (2 μl) of concentrated dye solution (2.5—5 mM) were added to a DNA sample (about 0.2 mM) by means of microsyringe without removing the solution from the viscometer. Measurements were repeated after each dye addition until reproducible flow times were observed. The relative viscosity ratios of the DNA-dye complex and the DNA were calculated using the expression $\eta/\eta_0 = \frac{t-t_0}{t_{DNA}-t_0}$, where t_0 is the flow time of the buffer; t and t_{DNA} are the flow times of the DNA sample in the presence and in the absence of the dye, respectively.

Electrochemical Measurements. The redox potential were determined by cyclic voltammery (CV) and differential pulse voltammetry (DPV) with a BAS Model CV-50W electrochemical system using ca. 1 mM solution of dye in a water and water/DMSO mixture (7 : 3 v/v) in the presence of supporting electrolytes, 0.1 M KCl and 0.1 M TBAP (tetrabutylammonium perchlorate), respectively. Measurements were conducted at 25 °C using the conventional design of a three-electrode system with a platinum wire counter electrode, an Ag/AgCl reference electrode, and a glassy carbon or disc gold working electrode (electrode areas of 7 and 2 mm^2, respectively). The voltammograms were recorded using a varying scan rate (2—200 mV s^{-1}) and the slope of the log–log dependence of the peak current vs. scan speed was considered as to be a measure of the diffusion-controlled process. Methyl viologen was used as a reference compound ($E^{2+/+} = -0.45$ V vs. SHE[23]).

Photocleavage Experiments. For the time dependence, samples having a volume of 100 μl containing 50 μM pBR322, 2 μM dye, and 10 mM Tris-HCL buffer (pH 7.3) were irradiated with a 500 W high-pressure mercury lamp (Ushio) equipped with a 310 nm cut-off filter (Toshiba UV-31). Sample solutions in 1.5 ml Eppendorf tubes were immersed in an ice-water bath and exposed to a light beam 30 cm from the light source (output ca. 30 mW cm^{-2}). Aliquots of 10 μl were removed at desired time intervals, extracted with phenol, and resolved by agarose gel electrophoresis (1% agarose) using a PBE running buffer (90 mM Tris, 2.5 mM EDTA, 90 mM boric acid, pH 8.2) for 40 min at 100 V. After gel electrophoresis was complete, the DNA was stained with ethidium bromide (0.5 μg ml^{-1}) for 30 min, and the gels were photographed on a Polaroid film Polapan 3200B. A dye-concentration effect was investigated using the same procedure, except that the sample volume was 10 μl and a fixed irradiation time of 20 min was applied.

Topoisomerase I Unwinding Assay. Samples (10 μl) of supercoiled pBR322 (62 μM) with varying concentrations of dye (0—60 μM) were incubated in the dark in the presence of topoisomerase I (12.5 units) at 37 °C for 90 min in a buffer (pH 7.6) containing 35 mM Tris, 72 mM KCl, and 5 mM $MgCl_2$. After phenol extraction, samples were resolved by gel electrophoresis and visualized using the same procedure as that used in photocleavage experiments.

Results and Discussion

Spectral Properties. Freshly prepared solutions of distilbazolium dyes contained more than 95% of the *E,E* isomer, as indicated from an HPLC analysis and ^{1}H NMR (the coupling constant of olefinic protons was 16.5 Hz, characteristic for derivatives of *trans*-stilbene). Upon exposure to visible light, absorption spectrum of the aqueous solution of dye gradually changed, showing a blue shift of the long-wave absorption band and significant hypochromicity. The clear isosbestic point suggested only a two-component system. The same behavior was observed for all 1,4-benzene substituted dyes, and the effect of the alkyl chain structure was negligible. The expected pathway and products of photoisomerization presented in Fig. 1 were proved using the example of **6** by HPLC separation of the irradiated isomer mixture and independently by its NMR analysis (calculation of the ratio of *cis*- (J = 12 Hz) and *trans*-protons (J = 16.5 Hz)). Since only two isomers were detected after irradiation, the formation of the *Z,Z* isomer of 1,4-substituted derivatives was neglected under the experimental conditions used here. However, in the case of the 1,3-substituted derivative, **10**, a third peak appeared in the chromatogram, which could be related to the *Z,Z* isomer, although it was not further proved.

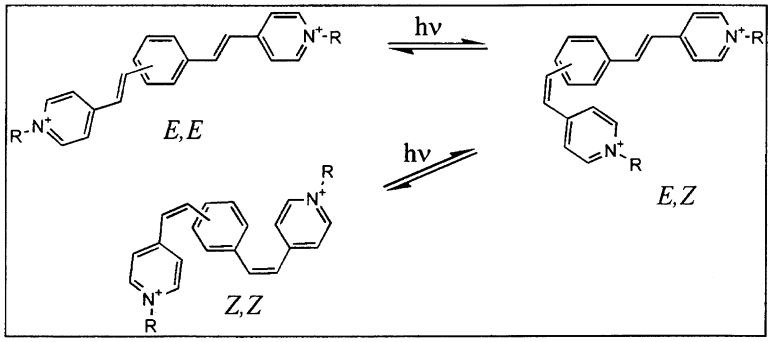

Fig. 1. Photoisomerization scheme of distilbazolium ligands.

The composition of the isomer mixture varied with the wavelength of the irradiation light; also, at a given λ, the concentration in the photostationary state (pss) of the *E,E*- and *E,Z*-isomers (abbreviated hereafter simply as *trans* and *cis*, respectively) should be governed by

$$\phi_{TC}\varepsilon_T c_T = \phi_{CT}\varepsilon_C c_C, \quad (1)$$

where ϕ_{TC} and ϕ_{CT} are the quantum yields of *trans*→*cis* and *cis*→*trans* isomerization, respectively, ε denotes the molar absorptivity, and subscripts T and C refer to the *trans* and *cis* isomers. Although a detailed discussion of the photoisomerization process will be reported elsewhere,[20] it is important to point out here that irradiation at a wavelength longer than λ_{iso} produced the *cis* isomer, and consequently, under illumination at $\lambda < \lambda_{iso}$ the *trans* isomer prevailed. The pss was generally reached after 20—30 min of irradiation (3—20 μM of dye) in the cell compartment of a spectrofluorimeter equipped with a 150 W Xe lamp.

The absorption spectra of particular isomers of distilbazolium dyes, obtained after HPLC separation with diode array detection, are shown in Fig. 2. The spectra of *trans* isomers possess virtually the same characteristics as the spectra of solutions before exposure to light, which confirmed the presence of only the *trans* isomer in freshly prepared solutions. Interestingly, the character of the substituent in a series of 1,4-derivatives did not significantly affect the spectral characteristics. All of the dyes exhibited similar molar absorptivities, and the position of absorption bands varied only slightly. An effect involving counter anions on the spectral properties of dyes, examined on the iodide, bromide, and hexafluorophosphate salts of **10** (compounds **10a**, **10b**, and **10c**, respectively) also appeared to be negligible, thus suggesting the absence of charge-transfer interactions, in agreement with the data reported for similar systems.[24]

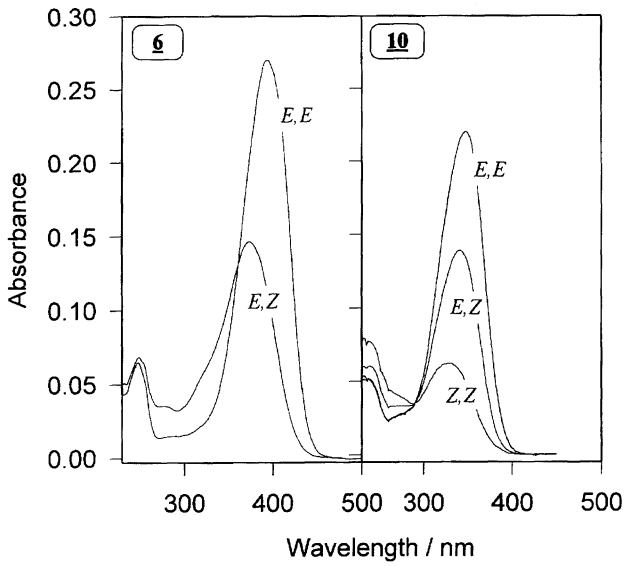

Fig. 2. Absorption spectra of isomers of **6** and **10** recorded with diode array detection after HPLC separation. The spectra were normalized to the dye concentration of 3.5 μM.

Table 1. Spectral Properties of Photoisomers of Distilbazolium Ligands in Aqueous Solution (HEPES Buffer pH 7.2)

	Absorption		Emission
	λ_{max}/nm ($\varepsilon \times 10^{-4}$/mol^{-1} dm^3 cm^{-1})		λ_{max}/nm (ϕ)[a]
Dye	*trans* isomer	*cis* isomer	*trans* isomer
6, **7**, **8**, **9**	394 (6.9)	371 (3.9)	480 (0.053)
10	349 (5.8)	341 (3.6)	460 (0.009)
Reference[b]	344 (3.3)	330 (0.9)	Weak

a) quantum yield of *trans* isomer, b) 4-[2-(1-methylpyridinium)-vinyl]-benzene in acetonitrile.[26]

The spectral parameters of the individual isomers are collected in Table 1. The absorption properties of isomeric dyes with different positions of the pyridiniumvinyl groups in the benzene ring coincide with the degree of delocalization of π-electrons in the molecules; the observed changes are in accordance with similar systems, 1,4- and 1,3-distyrylbenzenes.[25] As the result of a lengthening of the conjugation chain in the 1,4-derivatives (vs. 1,3-isomer), the bathochromic shift and a hyperchromic effect can be observed in the absorption spectra (e.g., for *trans* isomers $\Delta\lambda = 55$ nm, H = 16%), along with a smaller Stokes shift and an increase in the quantum yield of the fluorescence (Fig. 3, Table 1). The 1,3-derivative (**10**) may be regarded as being a simple addition of two structural entities of a reference stilbazolium derivative with a common benzene nucleus. Therefore, the spectral properties of *trans* **10** resemble more closely those of the parent methyl stilbazolium ligand.[26] The absorption spectra were not affected by the light source of the Hitachi spectrophotometer, contrary to the more intensive Xe lamp in the spectrofluorimeter. Even using a very narrow excitation slit and a very fast scan speed, consecutive fluorescence scans revealed a

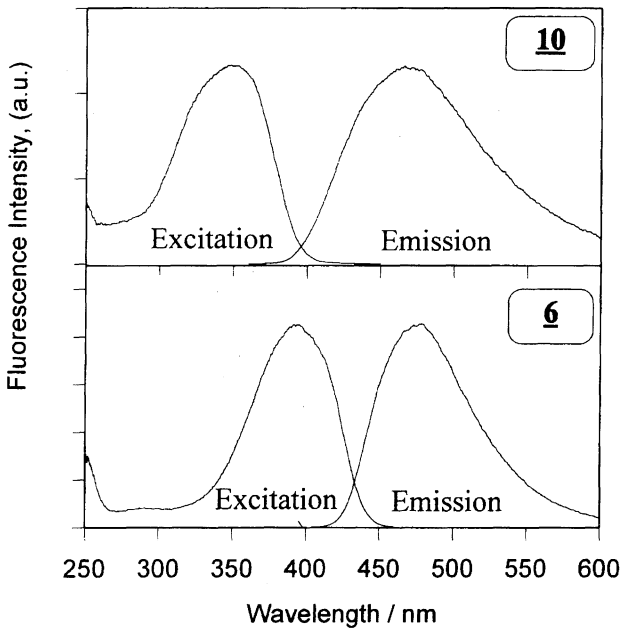

Fig. 3. Fluorescence excitation and emission spectra of aqueous solution of **10** and **6** ligands.

suppression of the emission signal, although no changes in the contour of the emission nor excitation bands were observed. The apparent light-induced quenching was ascribed to the formation of a weakly fluorescent *cis* isomer, since the original fluorescence could be restored upon subsequent irradiation at different wavelengths. The fluorescence quantum yield of the *cis* isomer was dramatically lower than that of *trans*; also, within the experimental error one can conclude that the *cis* isomer does not contribute to the observed fluorescence.

Electrochemical Properties. Similarity in the structural elements of the distilbazolium ligands to methyl viologen and related compounds, such as 1,2-bis(1-methylpyridinium-4-yl)ethylene, suggests a rather simple, two-step reduction mechanism, according to the following scheme:[27]

$$L^{2+} + e^- \overset{E_1}{\longleftrightarrow} L^{+\bullet} + e^- \overset{E_2}{\longleftrightarrow} L^0,$$

where L^{2+} stands for the dicationic ligand. This simple scheme may be valid for linear distilbazolium derivatives, where conjugation allows the formation of a neutral quinone form as a final reduction product;[27] however, in the case of a *meta*-substituted derivative, **10** one can suspect the formation of a biradical as a final product, as shown in Fig. 4. The formation of stable pyridinyl biradicals has already been evidenced for other bispyridinium-type compounds.[28]

Unfortunately, the redox properties of the investigated ligands seem to be more complex, since the recorded voltammograms exhibited a varying number of peaks, depending on the experimental conditions, such as the scan speed, recording potential range, and type of working electrode. On the other hand, the redox properties were not sensitive to changes in the character of counter anion (I^-, Br^-, or PF_6^-); moreover, the presence of DMSO (30%) in a sample solution and *trans–cis* photoisomerization also did not affect the redox characteristics.

Examples of the obtained voltammograms recorded with a scan speed of 100 mV s^{-1} are shown in Fig. 5, and the corresponding peak potentials (E^{red}, E^{ox}) and redox potentials obtained from DPV measurements (E) are collected in Table 2. The peaks listed in Table 2 were considered to be represen-

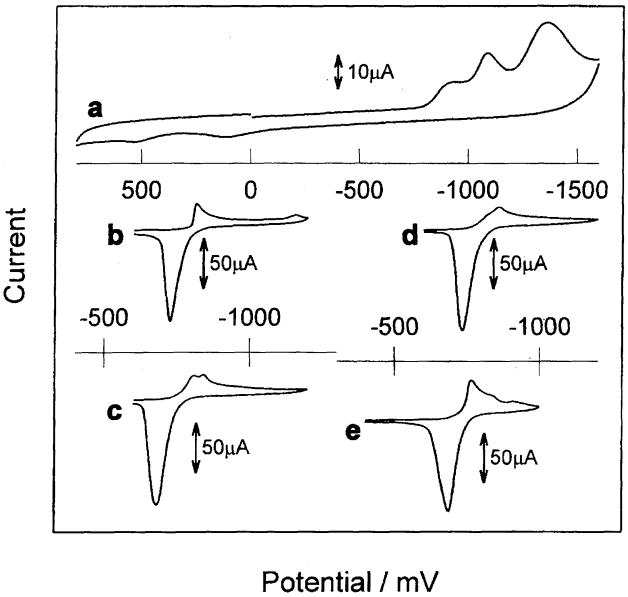

Fig. 5. Examples of cyclic voltammograms of 1 mM solutions of **10** (a), **6** (b), **8** (c), **7** (d), and **9** (d) recorded at 100 mV s^{-1} scan rate with glassy carbon working electrode.

Table 2. Cyclic Voltammetry Peak Potentials (E^{red}, E^{ox}) and Redox Potentials from Differential Pulse Voltammetry ($E_{1,2}$) for the Distilbazolim Ligands
Conditions: scan speed, 100 mV s^{-1}; temp, 25 °C; 0.1 M KCl supporting electrolyte; three electrode system: Ag/AgCl reference, Pt wire counter, and glassy carbon working electrode.

Dye	**10**	**6**	**7**	**8**	**9**
E_1^{red}/V	−0.91	−0.83	−0.81	−0.86	−0.77
E_2^{red}/V	−1.08	−1.17	−0.84	—	—
E_3^{red}/V	−1.34	—	—	—	—
E_1^{ox}/V	+0.10,	−0.74	−0.68	−0.76	−0.69
E_2^{ox}/V	+0.55	—	—	—	—
E_1/V	−0.92	−0.78	−0.76	−0.80	−0.74
E_2/V	−1.24	−1.11	—	—	—

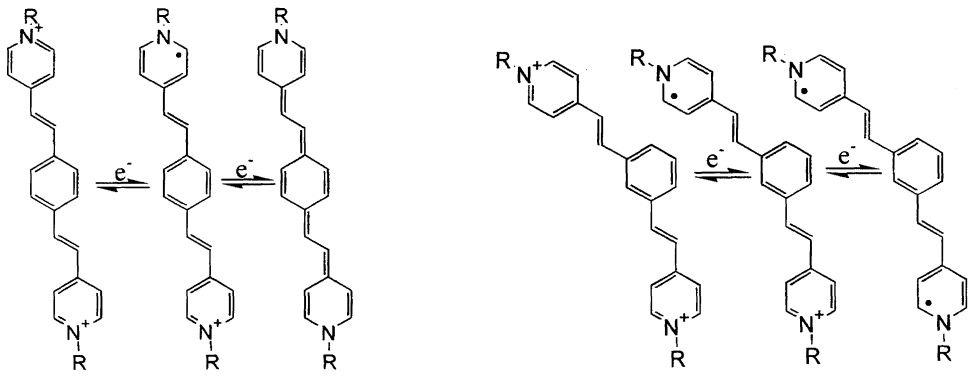

6 **10**

Fig. 4. Expected redox pathways for the highly conjugated linear derivatives (**6**), and weakly conjugated curved ligand (**10**).

tative of the redox behavior of the investigated compounds. Other, poorly reproducible variable peaks observed at low scan rates presumably originated from secondary reactions of the redox products. The possible reactions may involve dealkylation, dimerization or polymerization, as well as the formation of hydroxypyridinium derivatives or pyridones.[29,30] It should also be noted that during consecutive scans a gradual decrease in the redox response was observed for all compounds, suggesting the formation of an insulating film on the electrode surface. The dependencies of $\log i_p$ vs. log (scan rate) for the first reduction peak showed slopes close to 0.5, suggesting a diffusion-controlled process for all investigated dyes. A detailed discussion of the electrochemical results is beyond the scope of this paper; we wish to point out here only some common features and general conclusions.

The 1,3-substituted derivative, **10**, displays three reduction waves at −0.92, −1.08, and −1.34 V (the first two peaks may correspond to the same one-electron transfer process affected by adsorption phenomena), accompanied by two very weak oxidation waves at around +0.10 and +0.55 V (Fig. 5, scan a). A huge separation of the reduction and oxidation peaks suggests a highly irreversible redox behavior with possible contributions from chemical side-reactions (the postulated biradical species may be highly reactive). The reference stilbazolium derivative was reported to have a similar value of the redox potential (−0.99 V vs. SCE[26]), which proves a rather low degree of electronic conjugation in **10**.

Contrary to the meta derivative, 1,4-substituted linear compounds showed a higher degree of electrochemical reversibility, as can be inferred from the presence of strong oxidation peaks and their positions for individual derivatives (Fig. 5, scans b—e; Table 2). Surprisingly, the variation in the character of an alkyl substituent produced noticeable differences in the redox behavior of the dyes. The methyl derivative **6** showed two well-separated reduction peaks (Fig. 5, scans b); in the case of other compounds, only one reduction peak was observed, thus suggesting a two-electron transfer process. A single, well-developed oxidation peak was present for all para-derivatives; this peak was separated by 100—120 mV from its reduction counterpart, thus suggesting a rather slow, two-electron transfer process with E_1^{ox} being more negative than E_2^{ox}. The reduced, neutral quinone form of dye (Fig. 4) appeared to be sufficiently stable, giving a chemically reversible system. A disproportionation reaction could account for the instability of the cation radial.

Concluding, the redox behavior of the distilbazolium ligands depends on the substitution mode of the benzene ring, resulting in highly irreversible electrochemical properties in the case of the 1,3-derivative, and a far better reversibility observed for conjugated 1,4- derivatives. Since the oxidizing features of the dye are essential for their expected photocleavage activity towards DNA, we have evaluated the feasibility of such process for *N*-methyl derivatives of 1,3- and 1,4-substituted dyes using the Weller equation.[31]

$$E(^1D^{2+}/D^+) = E(D^{2+}/D^+) + h\nu_{00},$$

where $E(^1D^{2+}/D^+)$ is the reduction potential of the lowest excited state and $h\nu_{00}$ is the energy of the 0–0 transition of dye. The obtained values, +2.21 and +2.03, for **10** and **6**, respectively, indicate that the oxidation power of photoexcited dyes may be sufficient to facilitate photoinduced electron transfer from DNA bases (guanine) to the excited dye molecule.

DNA-Binding Properties. In the presence of nucleic acids, although all dyes exhibited significant hypochromicity, the extent depended on the concentration and base-pair composition of the oligonucleotide. The binding characteristics reported earlier for an isomeric mixture of unknown composition[15,16] were reexamined here under controlled conditions (in dark), so as to avoid any photoisomerization of the dye during titration. The investigations were limited to methyl substituent-containing dyes, **10** and **6**. Figures 6a and 6b show typical absorption spectra recorded during titration with the *trans* isomer of **6**. It should be noted that all of the dyes exhibited a similar tendency in spectra changes upon binding to nucleic acids. The interaction with [poly(dG-dC)]$_2$ (Fig. 6a) produced substantial hypochromicity (ca. 30%) and a rather small red shift of the absorption maximum. An isosbestic point was clearly recognized at 369 and 420 nm for **10** and **6**, respectively. Such a behavior is commonly observed for dyes undergoing intercalation,[11—14] thus suggesting an intercalation binding mode also in the case of these ligands. It is a commonly accepted feature of [poly(dG-dC)]$_2$ that the presence of NH_2 groups of guanine in the minor groove hampers the binding of ligands to the minor groove, and promotes intercalation.[2] The spectral changes during titration with [poly(dA-dT)]$_2$ were distinctly different, as can be seen from Fig. 6b and Table 3. The hypochromicity was less pronounced (ca. 10%) and the isosbestic points for **10** and **6** were observed at 357 and 406 nm, respectively. We assigned these spectral changes as indicative of the groove binding mode.

Studies of the effect of photoisomerization of the dye on the DNA-binding properties were limited to the **6** ligand because **10** showed a more complex photoisomerization behavior, as discussed earlier (three component system). One could expect that after isomerization of the *trans* isomer to the *cis* form (*E,Z* isomer with nonplanar structure, Fig. 1) the DNA-binding affinity should be dramatically affected. Unexpectedly, the *cis* isomer underwent similar spectral changes upon the addition of DNA, as did the *trans* isomer, except that the positions of the band maxima and the isosbestic points were shifted to the blue in accordance with the free *cis* isomer spectrum (Figs. 6c and 6d). One should remember that

Table 3. Spectral Properties of the Complexes of *cis* (*E,Z*) and *trans* (*E,E*) Isomers of **6** with Nucleic Acids

	[poly(dA-dT)]$_2$		[poly(dG-dC)]$_2$	
	cis	*trans*	*cis*	*trans*
λ_{iso}/nm	388	406	402	420
λ_{max}/nm	389	402	393	407
H/%	8	12	26	30

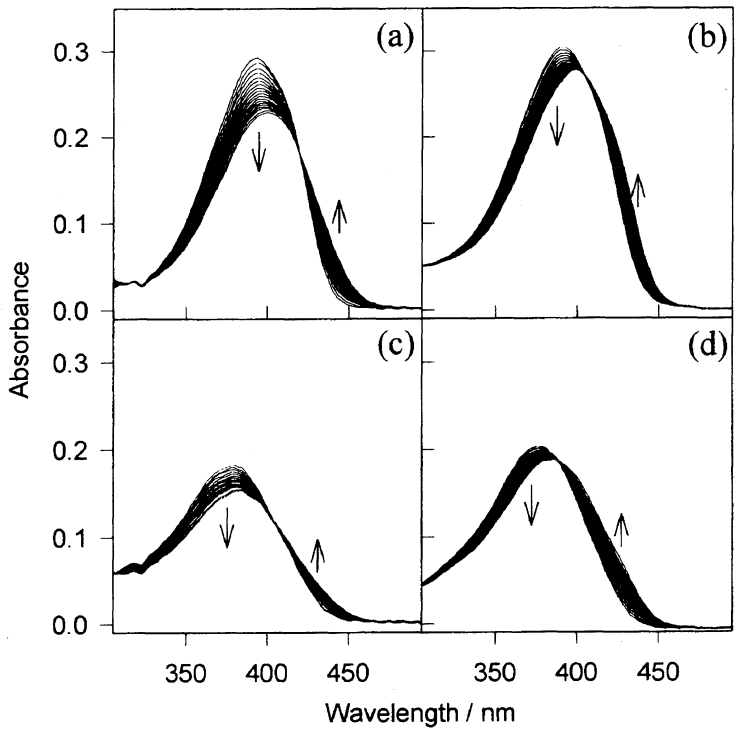

Fig. 6. Spectrophotometric titration of **6** isomers with nucleic acids. Conditions: [dye] = 5 μM, [oligonucleotide] = 0—250 μM, [NaCl] = 50 mM, HEPES buffer (10 mM, pH 7.2); (a) *trans* isomer/[poly(dG-dC)]$_2$, (b) *trans* isomer/[poly(dA-dT)]$_2$, (c) *cis* isomer/[poly(dG-dC)]$_2$, (d) *cis* isomer/[poly(dA-dT)]$_2$.

the sample labeled "*cis* isomer" does not represent a pure isomeric composition, but contains 80% of the *cis* isomer and 20% of the *trans* form. To extract the spectral features of the pure *cis* isomer we corrected the titration spectra, as described in Experimental.

The titration data were analyzed in order to extract the DNA-binding parameters. Binding isotherms were constructed according to the simple Scatchard method,[21] as well as to the site-exclusion McGhee-von Hippel model.[22] The experimental data could be fitted into both models showing a rather low degree of deviation from linearity. Unfortunately, small absorbance changes during titration with the *cis* isomer and additional errors connected with the absorbance correction resulted in some uncertainties of the fitting procedure; therefore, the binding parameters for complexes with the *cis* isomer contain a relatively big error. Examples of calculated binding parameters obtained in the presence of 50 mM NaCl are given in Table 4.

Table 4. Parameters for the Binding of Distilbazolium Ligands to Nucleic Acids Calculated Using the Site-Exclusion Model[22]
(K, binding constant; n, number of base pairs excluded by the bound ligand).
Conditions: 10 mM HEPES buffer pH 7.2, 50 mM NaCl.

Ligand	Isomer	$K\times10^{-5}$ (M^{-1}) n	
		[poly(dG-dC)]$_2$	[poly(dA-dT)]$_2$
10	*trans*	1.1±0.1, 2.4 (3.3±0.1)[a]	73±6, 5.4 (120±20)[a]
6	*trans*	0.67±0.1, 3.2 (4.1±0.5)[a]	2.1±0.3, 3.3 (8.5±0.5)[a]
6	*cis*	0.43±0.1, 3.0 (2.2±0.5)[a]	1.2±0.4, 5.3 (3.9±0.9)[a]

a) binding constant according to Scatchard model.[21]

A complex of **10** with [poly(dA-dT)]$_2$ exhibits a superior stability at about 70- and 20-times higher binding constant compared to the **10**/[poly(dG-dC)]$_2$ and **6**/[poly(dA-dT)]$_2$ systems, respectively. Such AT-binding preferences for ligands with a curved shape were commonly observed in the case of DAPI and Wilson's dyes containing unfused aromatic rings, and were ascribed to a favorable fit of the ligand into the minor groove curvature and feasibility of hydrogen-bond formation between the ligand and the DNA bases.[11,12,14] Since distilbazolium dyes cannot form stabilizing hydrogen bonds with the DNA minor groove, hydrophobic interactions seem to be the crucial factor contributing to the driving force responsible for complex formation. Electrostatic attractions may not be very essential, since ligand **6**, possessing the same positive charge, binds to [poly(dA-dT)]$_2$ with significantly lower affinity. One can suspect that ligand **6** is too long to be completely buried in the minor groove, and one of its ends may stick out from the minor groove. Such a binding mode can also explain the rather minor difference in the binding affinities of the *trans* and *cis* isomers of **6** with the AT polymer. The protruding part of the dye probably has enough space in the minor groove to undergo *trans–cis* isomerization without causing any dramatic changes to the stability

of complex. On the other hand, the intercalation complexes formed with the GC polymer seem to be even less sensitive to changes in the ligand structure. The similarity in the binding affinity of so structurally different ligands strongly suggests that in all cases the same part of the dye molecule interacts with DNA, and that this process may be considered to be a non-classical intercalation. All three dyes (*trans*-**10**, *trans*-**6**, and *cis*-**6**) have a common planar element consisting of one pyridinium ring linked with a benzene moiety by a *trans*-vinyl bridge. The size of this element probably fits to the intercalation pocket, thus allowing an efficient stacking interaction of the aromatic rings of the dye with the DNA base pairs. The remaining part of the dye molecule may be located both in a minor or in a major groove, and can undergo isomerization. Small effects on the binding affinity of the substitution mode of the benzene ring and changes in the planarity caused by isomerization are consistent with this model, suggesting that the interaction of DNA with this external part of the dye is rather weak.

To examine the influence of the ionic strength, the effect of the NaCl concentration on the binding parameters was studied; the results are presented in Fig. 7. According to counterion condensation theory, log K versus log c_{NaCl} should give a linear dependence with the slope corresponding to the number of Na^+ ions released per bound ligand molecule.[32,33] The observed values of slopes, 1.8±0.1, and 0.9±0.1, for GC and AT complexes, respectively, seem to depend on the base composition of the biopolymer exclusively, and are not affected by the benzene substitution mode nor by isomerization. The slopes for [poly(dG-dC)]$_2$ complexes are close to the value of 2 predicted for dicationic ligand interacting with DNA. Interestingly, the salt dependencies for AT complexes with slopes of close to 1 suggest complexation involving only one charge in the interactions with DNA. Since the minor groove is responsible for the interaction of the ligand with the AT polymer, this result is rather surprising, because one can expect an effective neutralization of both charges of the ligand by phosphate groups, since the ligands lay along the negatively charged groove. Moreover, changes in the geometrical distribution of positive charges in the ligand molecule caused by isomerization should also affect its electrostatic interactions with DNA phosphate groups (from the molecular modeling calculation the distances between pyridinium nitrogens in *trans* and *cis* **6** are 15.5 and 12.8 Å, respectively); however, these simple expectations were not reflected in the experimental observation. The low values of the slopes for dye/AT systems may result from an incomplete insertion of dye into the minor grove, or may be caused by an efficient charge delocalization within the entire molecule, which hampers an efficient electrostatic interaction with localized negative charges on the phosphate groups. Indeed, a molecular-modeling calculation confirmed this, showing that the effective charge on pyridinium nitrogens is only +0.045, and that this value is not sensitive to the extent of the π-electron conjugation (**10** vs. **6**) nor to isomerization. In the case of the GC polymer, the higher slope may be accounted for the additional charge-transfer interaction between the intercalated ligand and guanine; some evidence of such interactions was obtained from a quenching study of ligand fluorescence in the presence of the GC polymer, which is discussed later. On the other hand, the ligand residing in the minor groove at AT sequences is rather shielded from such stacking interactions with DNA bases. The practical outcome from the ionic-strength effect shown in Fig. 7 is that although at low salt concentration the affinity of the **6** ligand to the both polymers is comparable, a higher salt content suppresses the binding of **6** to GC sites, while the effect is minor for its binding to AT sites.

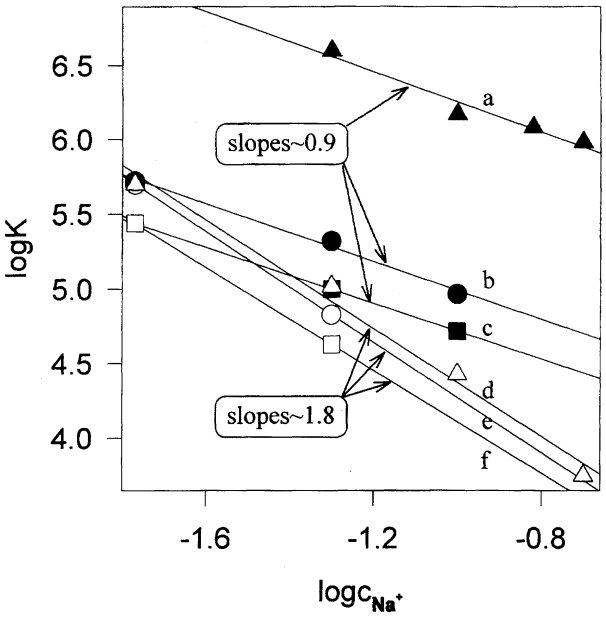

Fig. 7. Salt effect on the binding affinity of distilbazolium ligands to DNA: *trans* **10**/[poly(dA-dT)]$_2$ (a), *trans* **6**/[poly(dA-dT)]$_2$ (b), *cis* **6**/[poly(dA-dT)]$_2$ (c), *trans* **10**/[poly(dG-dC)]$_2$ (d), *trans* **6**/[poly(dG-dC)]$_2$ (e), *cis* **6**/[poly(dG-dC)]$_2$ (f).

Fluorescence Properties of Ligand–DNA Complexes and the Photocleavage of DNA. Efforts to use a fluorescence technique for an alternative evaluation of the binding affinity ended in failure because of the already mentioned problems, concerning the photoisomerization of ligands exposed to the excitation light. Nevertheless, an inspection of the fluorescence spectra and titration data from carefully conducted experiments could still provide some valuable information. During titration of the dye, no spectral shift of the emission band was observed upon the addition of GC and AT polymers or calf thymus DNA. The only effect observed for particular dyes was that the fluorescence intensity varied depending on the type of DNA and its concentration.

Typical fluorescence dependencies on the DNA concentration are presented in Fig. 8. It should be noted that these titration data were collected with a sample solution initially containing only the *trans* form of the dye, and that the time of illumination of the sample with excitation light was comparable in each titration experiment. In all systems, although the position and shape of the emission band were virtually insen-

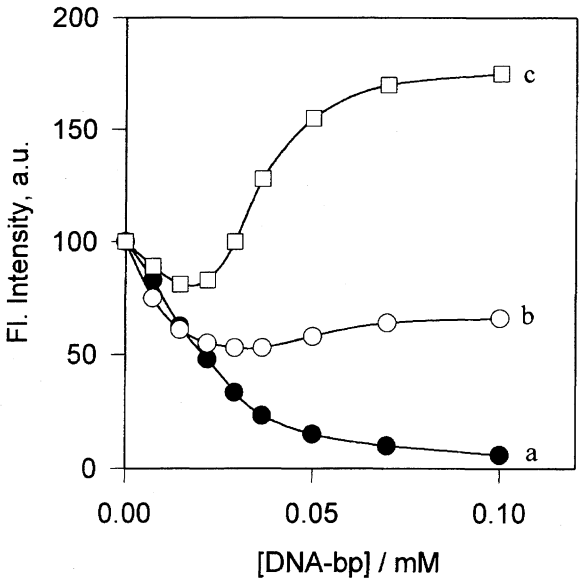

Fig. 8. Effect of DNA concentration on the fluorescence intensity of distilbazolium ligands: **10**/[poly(dG-dC)]$_2$ (a), **6**/[poly(dG-dC)]$_2$ (b), **6**/[poly(dA-dT)]$_2$ (c); [dye] = 2 μM.

sitive to the DNA concentration, the fluorescence intensity varied significantly. At low DNA concentration, each system showed a decrease in the fluorescence. The quenching continued at higher DNA concentrations for the GC polymer (Fig. 8, curves a and b), whereas [poly(dA-dT)]$_2$ at a higher DNA concentration first caused a restoration and next even an enhancement of the emission (Fig. 8, curve c).

The **10**-GC complex undergoes significant quenching along with an increase in the DNA concentration, contrary to the **6**-GC complex, which showed rather modest quenching. The initial (low DNA concentration) decrease in the dye emission was explained in our earlier work[16] by intercalation (guanine or adenine quenching) and by the possibility of aggregation of the dye upon binding to DNA. The vulnerability of the dyes to undergo *trans–cis* isomerization in the presence of light strongly suggests that photoisomerization may serve as a main source of the fluorescence changes observed in the system. Undoubtedly, all of these processes overlap, and result in the fluorescence changes; however, if one excludes aggregation phenomena, the discussion should involve a four-component system with *trans* and *cis* isomers free in solution and bound to DNA. When one considers, for example, fluorescence changes in the presence of the AT polymer (Fig. 8, curve c), it is easy to predict that light enhances the formation of a weakly fluorescent *cis* isomer of the free ligand, and simultaneously DNA addition results in the formation of DNA–ligand complexes with rather higher emission properties (the dye molecule is buried into the minor groove, and is thus protected from rotational or torsional quenching, processes which prevail for free dyes[34]). The first process is supposed to prevail at low DNA concentration where an excess of free ligand is assumed; this causes an apparent fluorescence quenching. A further enhancement of the fluorescence is in agreement with the formation of a *trans* isomer–DNA complex, which is more stable (Table 4) and exhibits a higher quantum yield.

Contrary to linear derivatives (e.g., **6**), which at least partially restored their initial fluorescence intensity at higher P/D ratios (Fig. 8, curve b), ligand **10** once more showed a different behavior, exhibiting only monotonous quenching along with an increase in the DNA concentration. Finally, the fluorescence quantum yield of **10** was deteriorated by a factor of 5 at a P/D ratio equal to 20. The differences in the quenching behavior of linear and curved derivatives may be rationalized in terms of the probability of photoinduced electron transfer to take place. The driving force of photoinduced electron transfer for a guanine-dye couple is expected to be superior for **10**, as already discussed.

A confirmation of the feasibility of such a process was provided by preliminary experiments with a photocleavage of circular DNA, pBR322. The conversion of supercoiled circular DNA (form I) into nicked (form II) and into linear DNA is regarded as evidence of cleavage activity of the dye. Figure 9 shows the results obtained after gel-electrophoresis separation of the photocleavage products in the presence of **10**. Since the starting supercoiled DNA was not purified prior to use, it also contained a small fraction of the nicked form, as indicated from lanes 5, 6, and 12 in Fig. 9. The irradiation of DNA in the absence of a dye did not produce any noticeable changes in the relative intensities of the bands

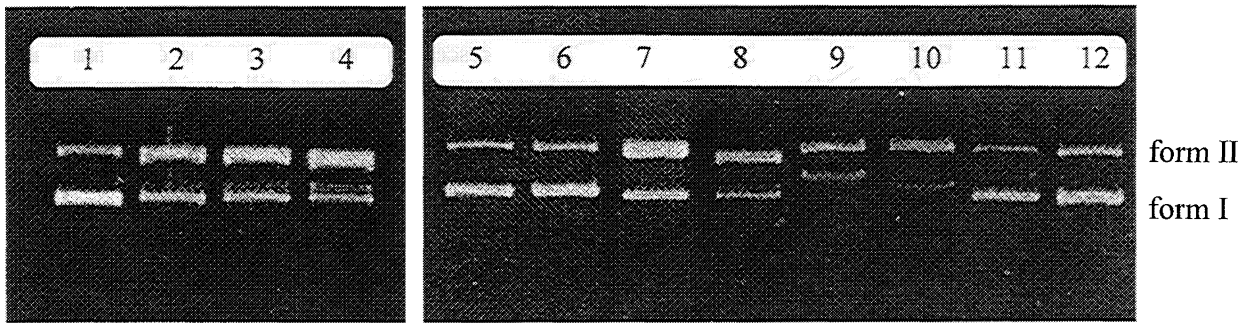

Fig. 9. Photocleavage of supercoiled cDNA pBR322 by **10**. Lanes 1—4: 50 μM DNA and 2 μM of **10**, irradiation time was 0, 10, 20, and 40 min, respectively. Lanes 5, 6, and 12: 50 μM DNA in the absence of dye, irradiated for 20 min (6 and 12), in the dark (5). Lanes 7—10: 50 μM DNA and **10** at varied concentration irradiated for 20 min; dye concentrations were: 2, 10, 15, and 25 μM, respectively. Lane 11: 50 μM DNA and 25 μM of **10** in the dark. Forms I and II denote supercoiled and nicked cDNA, respectively.

corresponding to both DNA forms (Fig. 9, lanes 5 vs. lanes 6 and 12). The incubation of DNA with a dye in the dark did not cause any substantial changes either (Fig. 9, lanes 1 and 4). On the contrary, the irradiation of a DNA-dye mixture resulted in a relative weakening of the band representing supercoiled cDNA (form I), and an enhancement of the band of relaxed DNA (form II). The observed effects are undoubtedly caused by a cleavage of one strand of the double-stranded DNA by a photoexcited dye molecule, thus making a relaxed supercoiled cDNA. The prolonged time of irradiation enhanced the nicking of supercoiled cDNA, as is illustrated by lanes 1—4 in Fig. 9. The cleavage efficiency also depended on the dye concentration; the degradation of DNA increased at higher dye/DNA ratios (Fig. 9, lanes 7—10). It should be noted that while both **6** and **10** interacted with supercoiled circular DNA and caused photocleavage, the latter dye appeared to be more efficient. Although it is too early to derive any cleavage mechanism, there is a coincidence between the cleavage efficiency and the fluorescence quenching rate observed in the presence of DNA. This may suggest the importance of an electron-transfer process between the guanine and the photoexcited dye; however, to fully understand the mechanism, including the structural features of the isomers, further studies are needed.

Circular Dichroism Measurements Free bis[2-(1-alkylpyridinium-4-yl)vinyl]benzene ligands have no intrinsic CD activity; however, upon binding to DNA, the induced CD spectrum (ICD) of the ligand may appear, and its characteristics reflect the binding mode. Figure 10 shows the CD spectra of **10** complexes with AT and GC polymers. Those for other ligands exhibited similar characteristics, except that the ICD bands were shifted to the red and their intensities were lower. The spectral range below 300 nm contains CD bands of DNA, and are not discussed here. The dramatic difference between complexes with AT (Fig. 10, spectra a, b, and c) and GC polymers (Fig. 10, spectrum d) is evident in the diagnostic region where only the dye absorbs (300—400 nm). The strong positive ICD signal observed in the presence of [poly(dA-dT)]$_2$ is undoubtedly caused by a groove-binding process. Similar positive ICD spectra were assigned to this binding mode for a DAPI (4′,6-diamidino-2-phenylindole) complex with the AT polymer and for other structurally similar ligands.[12,35,36] Intercalation is expected to be manifested by a weak bisignate spectrum with positive and negative parts, whose position depends on the geometry of the ligand in the intercalation pocket; however, in many cases no ICD was detected for intercalated ligands.[12] Therefore, the lack of ICD observed for the **10**/[poly(dG-dC)]$_2$ complex strongly suggests that intercalation is involved in this binding mode. The possibility of external binding of the dye should be rather ruled out, since this type of interaction results in the stacking of dye molecules, and should produce significant exciton interactions, which usually lead to the development of an extra, strong positive CD band at the red end of the dye absorption band. Such exciton bands were reported for some groove bound ligands at low P/D ratios (excess of the dye). We did not observe any evidence of exciton bands in both the presence of the AT and GC polymers (Fig. 10). The ICD signal at 360 nm gradually increased along with the concentration of DNA, and the shape of the spectra was virtually the same at both low and high P/D ratios (Fig. 10, spectra a, b, and c).

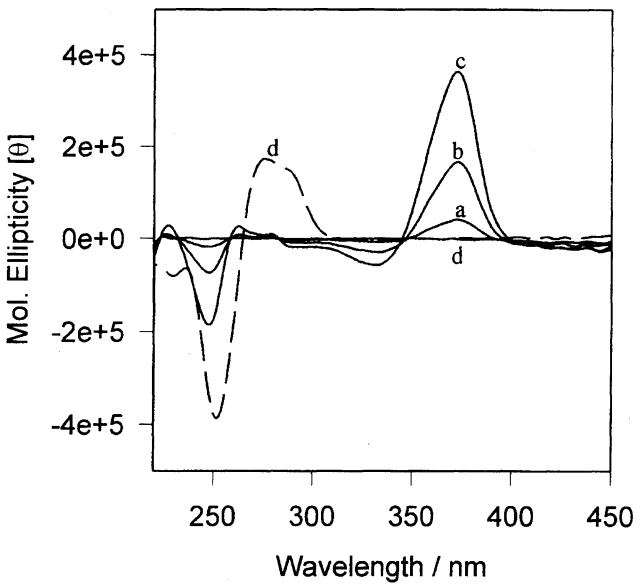

Fig. 10. Circular dichroism spectra of **10**/[poly(dA-dT)]$_2$ complex (solid line, a—c), and **10**/[poly(dG-dC)]$_2$ complex (broken line, d): DNA concn, 3 μM (a), 25 μM (b), 50 μM (c and d). Conditions: [dye] = 5 μM, 10 mM HEPES buffer (pH 7.0), 50 mM NaCl, temp = 30 °C.

All of the CD data so far discussed were obtained with solutions prepared from a *trans* isomer of dyes. The following question arises: How does photoisomerization affect the ICD spectra? The absorption spectra of the DNA-bound *trans* isomer is red shifted compared to the *cis* isomer; thus, if the *cis* isomer is also bound to the minor groove, its blue-shifted ICD should appear. Unexpectedly, the CD spectra recorded for *trans* **6** and a *cis*/*trans* mixture of **6** (8 : 2) in the presence of the AT polymer were virtually the same. Any explanation of this should involve the effect of the light source applied during a CD measurement. The spectrometer was equipped with a 450 W Xe lamp strong enough to change the isomeric composition of the sample solution during measurements if one considers the low scan speed necessary to reduce the noise level. The time of the sample exposure to light during the measurement (about 10 min) is sufficient to produce the same photostationary state, regardless of the initial isomeric composition of the sample.

Unwinding of Supercoiled cDNA. To further prove the validity of the assigned intercalation binding mode at GC sequences, viscometric titrations were carried out using supercoiled plasmid DNA, [poly(dG-dC)]$_2$, and [poly(dA-dT)]$_2$. The reference ligands, ethidium bromide (EB) and Hoechst 33258, which are known to be a typical intercalator and groove binder, respectively, were also tested. The increase in the viscosity of the solution reflects the increase in the DNA contour length upon ligand binding, and is gen-

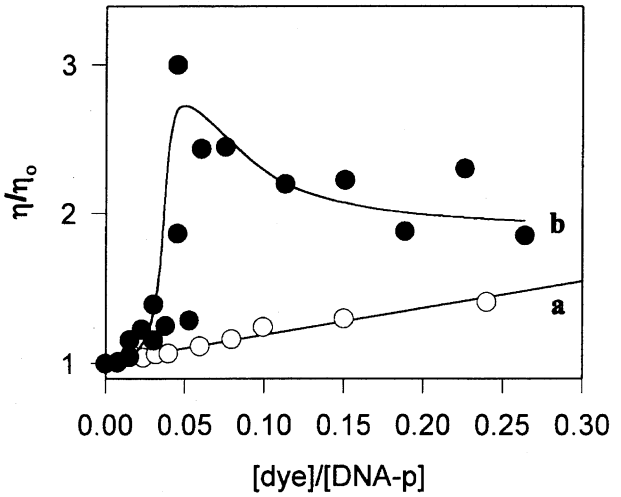

Fig. 11. Viscometric titration of $[poly(dG\text{-}dC)]_2$ (a) and supercoiled circular DNA (b) with **10**. Conditions: [DNA] = 0.22 mM, 10 mM HEPES (pH 7.2), temp = 30 °C.

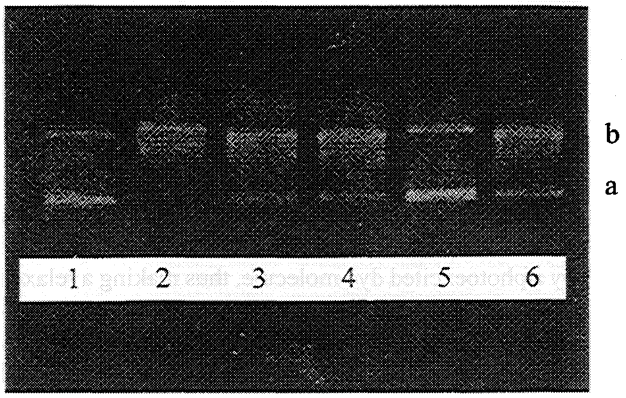

Fig. 12. Agarose gel electrophoresis of supercoiled cDNA pBR 322, unwound by topoisomerase I. Lanes 1 and 2 contain unrelaxed pBR 322 and relaxed by topoisomerase I, repsectively. DNA in lanes 3—6 were relaxed by topoisomerase I in the presence of 0.6, 3.0, 6.0, and 30 μM of **6**, respectively. Bands a and b denote supercoiled and relaxed cDNA, respectively.

erally regarded as being evidence of intercalation.[37] On the other hand, groove binding does not give rise to an increase in the viscosity. The binding of distilbazolium ligands in the present study with the AT polymer did not cause any increase in viscosity, as expected for its groove-binding mode; this was the case for the reference compound, Hoechst 33258. On the contrary, the titration of plasmid DNA and the GC polymer produced a substantial increase in the specific viscosity, as illustrated in Fig. 11. Both dyes, **10** and **6** provided similar titration traces. A gradual increase in the specific viscosity during the titration of the GC polymer (Fig. 11, curve a) confirmed the ability of the ligands to unwind DNA by intercalation in the GC sites. A qualitatively similar behavior was observed for EB and **10**: The solution viscosity significantly increases as the dye DNA ratio increases, contrary to Hoechst 33258, whose addition caused a negligible variation in the viscosity. The titration of supercoiled DNA provided further evidence of the intercalating ability of **10** (Fig. 11, curve b). It showed an initial increase in the viscosity, which was followed by a decrease, thus clearly evidencing the DNA unwinding ability of **10**. Photoisomerization did not produced any noticeable differences in the titration profiles, which suggests that both isomers undergo intercalation in accordance with the model proposed earlier. The complexity of the base composition in natural DNA precludes any detailed discussion of the titration process. Despite the fact that groove binding at the AT sequences is much more favorable for **10** (Table 4), there is a possibility that AT/GC mixed sites in natural DNA may have lead to a preference for intercalation.

Further evidence of the unwinding of superhelical cDNA, pBR322, was provided by an experiment with topoisomerase I. In the absence of an intercalating ligand, topoisomerase I relaxes positively supercoiled cDNA, contrary to an intercalator-assisted assay, where the products of topoisomerase I action exhibit negative superhelicity.[38] As can be seen in Fig. 12, while the untreated sample of our supercoiled cDNA contained a small amount of nicked form (lane 1), after a treatment with the enzyme all of the supercoiled form was transformed into relaxed cDNA (lane 2). On the other hand, the assay in the presence of **6** indicates that the dye causes an unwinding of superhelical DNA in a concentration-dependent manner, as expected for intercalators (Fig. 12, lanes 3—6). The banding patterns were not well developed, probably as a result of the relatively high voltage used for band separation. Unfortunately, our electrophoresis instrumentation did not provide any flexible voltage variation option. Nevertheless, it is evident that **6** at a concentration of 6 μM, unwound supercoiled cDNA completely (Fig. 12, lane 5).

Conclusions

Bis[2-(1-alkylpyridinium-4-yl)vinyl]benzene ligands possess a number of promising positive features if one considers the requirements for a drug to be capable of performing several different functions upon binding to nucleic acids (e.g., recognition, probing, and cleaving). All of these observed features result from the unique structural, spectral, and electrochemical properties of the presented ligands. The capability of the ligands to undergo photoisomerization allows one to tune the structural features of the molecule (from a planar *trans* to three-dimensional *cis* form); the parameter, which plays an important role in ligand-DNA interactions, also results in easily observable spectral changes upon isomerization. The absorption characteristics and fluorescence of particular isomers have been found to significantly differ, which has an analytical potential for the base-sequence selective probing of DNA. All compounds showed electrochemical activity, which varied with the substitution mode on benzene, as well as with the character of alkyl substituents at pyridinium nitrogens. The primary redox activity combined with their photophysical features opened the possibility of observing the light-sensitized strand cleavage of DNA. Photocleavage by distilbazolium ligands occurs at neutral pH under irradiation by visible light, leading mainly to single-strand nicking of supercoiled circular DNA. Although dyes

interact with both the AT and GC sequences of DNA, the resulting complexes have different binding characteristics. A complex with AT sequences was attributed to an interaction of the dye with the minor groove of DNA, while an intercalation was proposed to be responsible for the interaction with GC sequences. Generally, interactions of distilbazolium ligands with DNA resemble those of DAPI and unfused-aromatic dications, despite the fact that in the case of distilbazolium dyes there is no possibility of hydrogen-bond formation. The minor-groove complexes at AT sequences have several distinguishable characteristics, such as lower hypochromicity of the absorption band upon complex formation, an intense, positive ICD peak of the dye, and an enhancement of the ligand fluorescence. On the contrary, complexes with GC sequences exhibit more pronounced hypochromicity, very weak CD activity in the range of the absorption band of the ligand, and efficient fluorescence quenching upon binding to DNA. Additional evidence for the importance of the intercalation binding mode was provided by viscometric titration and a topoisomerase I unwinding assay. Unexpectedly, a nonplanar *cis* isomer also binds to DNA with binding features resembling those of the *trans* isomer, although with lower affinity. To explain the similar binding features of both isomers, an interaction model has been proposed, where only a part of a dye molecule including a central benzene ring and one of the vinylpyridinium arms was assumed to strongly interact with DNA (minor groove at AT sequences or intercalation pocket at GC steps). The other vinylpyridinium arm, sticking out from the DNA groove, could undergo *trans–cis* isomerization without causing any dramatic effects on the binding equilibria.

Further work is currently in progress in order to investigate some aspects related to DNA-mediated photoisomerization, its importance in the photocleavage activity of dyes, and the analytical potential of photoisomerization for the DNA probing and detection.

The present study was partially supported by the Grant in Aid for Scientific Research from the Ministry of Education, Science and Culture.

References

1) W. D. Wilson, in "Nucleic Acids in Chemistry and Biology," ed by G. M. Blackburn and M. J. Gait, IRL Press, New York (1990).
2) W. D. Wilson and R. L. Jones, in "Intercalation Chemistry," ed by M. S. Whittingham and A. J. Jacobson, Academic Press, New York (1982).
3) A. J. Blacker, J. Jazwinski, J.-M. Lehn, and F. X. Wilhelm, *J. Chem. Soc., Chem. Commun.*, **1986**, 1035.
4) G. Colmenarejo, M. C. Guttierez-Alonso, M. Barcena, J. M. Kelly, J. Montero, and G. Orellana, *J. Biomol. Struct. Dyn.*, **12**, 827 (1995).
5) A. Slama-Schwok, J. Jazwinski, A. Bere, T. Montenay-Garestier, M. Rougee, C. Helene, and J.-M. Lehn, *Biochemistry*, **28**, 3234 (1989).
6) P. Fromherz and B. Rieger, *J. Am. Chem. Soc.*, **108**, 5361 (1986).
7) A. M. Brun and A. Harriman, *J. Am. Chem. Soc.*, **113**, 8153 (1991).
8) S. Takenaka, T. Ihara, and M. Takagi, *Chem. Lett.*, **1992**, 1.
9) C. Helene, T. Le Doan, and N. T. Thuong, in "Photochemical Probes in Biochemistry," ed by P. E. Nielsen, Kluwer Academic Publishers, Dorbrecht (1989), p. 219.
10) S. Takenaka, N. Shigemoto, and H. Kondo, *Supramol. Chem.*, **9**, 47 (1998).
11) W. D. Wilson, F. A. Tanious, H. J. Barton, R. Jones, L. Strekowski, and D. W. Boykin, *J. Am. Chem. Soc.*, **111**, 5008 (1989).
12) F. A. Tanious, J. Spychala, A. Kumar, K. Greene, D. W. Boykin, and W. D. Wilson, *J. Biomol. Struct. Dyn.*, **11**, 1063 (1994).
13) J. W. Lown, *Anti-Cancer Drug Des.*, **3**, 25 (1988).
14) A. Czarny, D. W. Boykin, A. A. Wood, C. M. Nunn, S. Neidle, M. Zhao, and W. D. Wilson, *J. Am. Chem. Soc.*, **117**, 4716 (1995).
15) B. Juskowiak, S. Takenaka, M. Takagi, and H. Kondo, *Nucl. Acids Symp. Ser.*, **37**, 265 (1997).
16) S. Takenaka, B. Juskowiak, K. Yuziriha, M. Takagi, K. Miyajima, and H. Kondo, *Anal. Sci.*, **13**, Suppl., 457 (1997).
17) M. J. Minch and S. S. Shah, *J. Chem. Educ.*, **54**, 709 (1977).
18) S. Takenaka, H. Sato, T. Ihara, and M. Takagi, *J. Heterocycl. Chem.*, **34**, 123 (1997).
19) J. N. Demas and G. Crosby, *J. Phys. Chem.*, **75**, 991 (1971).
20) B. Juskowiak, M. Sato, S. Takenaka, and M. Takagi, in preparation.
21) G. Scatchard, *Ann. N. Y. Acad. Sci.*, **51**, 660 (1949).
22) J. D. McGhee and P. H. von Hippel, *J. Mol. Biol.*, **86**, 469 (1974).
23) M. Ito and T. Kuwana, *J. Electroanal. Chem. Interfacial Electrochem.*, **32**, 415 (1971).
24) H. L. White and C. J. Cavallito, *Biochim. Biophys. Acta*, **206**, 242 (1970).
25) B. M. Krasovitskii and B. M. Bolotin, "Organic Luminescent Materials," VCH, Weinheim (1988), pp. 46—48.
26) K. Takagi and Y. Ogata, *J. Org. Chem.*, **47**, 1409 (1982).
27) S. Hunig, J. Gross, and W. Schenk, *Liebigs Ann. Chem.*, **1973**, 324.
28) M. Itoh and E. M. Kosower, *J. Am. Chem. Soc.*, **90**, 1843 (1968).
29) H. T. Van Dam and J. J. Ponjee, *J. Electrochem. Soc.*, **121**, 1555 (1974).
30) J. S. Bellin, R. Alexander, and R. D. Mahoney, *Photochem. Photobiol.*, **17**, 17 (1973).
31) D. Rehm and A. Weller, *Isr. J. Chem.*, **8**, 259 (1970).
32) G. S. Manning, *Q. Rev. Biophys.*, **2**, 179 (1978).
33) W. D. Wilson, C. R. Krishnamoorthy, Y. H. Wang, and J. C. Smith, *Biopolymers*, **24**, 1941 (1985).
34) B. Juskowiak, M. Sato, S. Takenaka, and M. Takagi, *Nucl. Acids Symp. Ser.*, **39**, 35 (1998).
35) W. D. Wilson, F. A. Tanious, H. J. Barton, R. L. Jones, K. Fox, R. L. Wydra, and L. Strekowski, *Biochemistry*, **29**, 8452 (1990).
36) K. Jansen, P. Lincoln, and B. Norden, *Biochemistry*, **32**, 6605 (1993).
37) G. Cohen and H. Eisenberg, *Biopolymers*, **8**, 45 (1969).
38) L. M. Fisher, R. Kuroda, and T. T. Sakai, *Biochemistry*, **24**, 3119 (1985).